Design and Synthesis of Some Novel Quinoline Derivatives as Anticancer and Radiosensitizing Agents Targeting VEGFR Tyrosine Kinase

Mostafa M. Ghorab,[a]* Fatma A. Ragab,[b] Helmy I. Heiba,[c] and Walid M. Ghorab[c]

[a]Medicinal, Aromatic and Poisonous Plants Research Center, College of Pharmacy, King Saud University, Riyadh,Saudi Arabia
[b]Department of Pharmaceutical Chemistry, Faculty of Pharmacy, Cairo University, Cairo, Egypt
[c]Department of Drug Radiation Research, National Centre for Radiation Research and Technology, Atomic Energy Authority, Nasr City, Cairo, Egypt
*E-mail: mmsghorab@yahoo.com

Received July 19, 2010
DOI 10.1002/jhet.749
Published online 27 July 2011 in Wiley Online Library (wileyonlinelibrary.com).

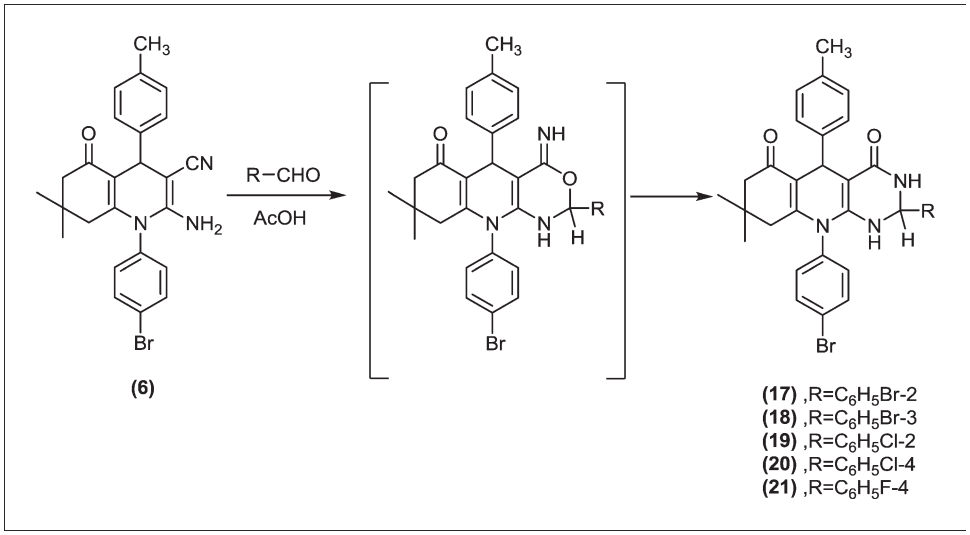

Quinoline derivatives posses many types of biological activities and have been reported to show significant anticancer activity. There is a variety of mechanisms for the anticancer activity and the most distinguished mechanism is the inhibition of vascular epithelial growth factor receptor tyrosine kinase (VEGFRTK). Novel quinoline derivatives **6–12** and pyrimido[4,5-*b*]quinoline derivatives **16–20** are reported herein. All the newly synthesized compounds were evaluated for their *in vitro* anticancer activity against human breast cancer cell line (MCF7) in which VEGFR is highly expressed. Compounds **6** and **7** with IC_{50} values of 8.5 μM and 21.9 μM were the most active compounds and exhibited cytotoxic activities higher than that of the reference drug doxorubicin (IC_{50} = 32.02 μM). The most active compounds **6** and **7** were further evaluated for their ability to enhance the cell killing effect of γ-radiation.

J. Heterocyclic Chem., **48**, 1269 (2011).

INTRODUCTION

Quinoline derivatives posses a wide range of biological activities including anti-inflammatory [1], antileishmanial [2], antifungal [3], antituberculosis [4], and antimalarial activities [5,6]. Also, several novel quinoline derivatives have been reported to show substantial anticancer activities [7–14].

It has been known that quinoline derivatives may act as anticancer agents through a variety of mechanisms such as cell cycle arrest in the G2 phase [13], topoisomerase inhibition [15], and inhibition of tubulin polymerization [16], and the most common mechanism was the inhibition of tyrosine kinases [17–19], specially vascular epithelial growth factor receptor tyrosine kinase (VEGFRTK) [20–22].

Protein tyrosine kinases are enzymes that provide a central switch mechanism in cellular signal transduction pathways. As such they are involved in many cellular processes such as cell proliferation, metabolism, survival, and apoptosis. Several protein tyrosine kinases are known to be activated in cancer cells and to drive tumor growth, angiogenesis, progression, and metastasis. Therefore, blocking tyrosine kinase activity represents a rational approach to cancer therapy [23].

The cancer cell is characterized by oncogene-derived tumor expression of pro-angiogenic proteins, such as vascular endothelial growth factor (VEGF), placenta-like growth factor, basic fibroblast growth factor, platelet-derived endothelial growth factor, angiopoietin-2,

Scheme 1

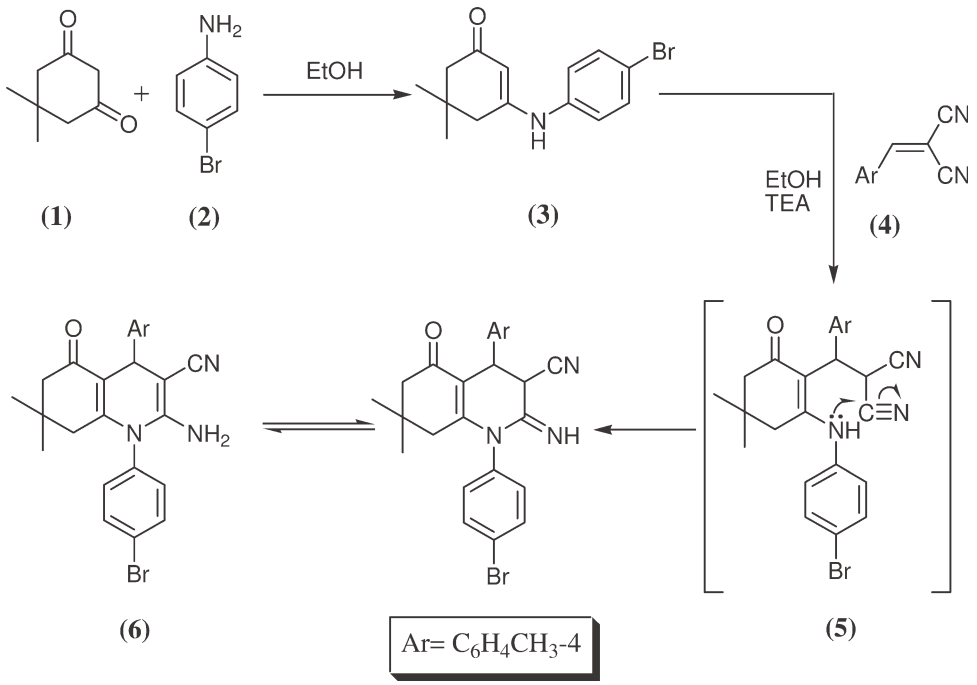

hepatocyte growth factor, and insulin-like growth factor [24]. The mentioned pro-angiogenic growth factors bind to specific receptors that possess receptor tyrosine kinase (RTK) activity.

Overexpression of VEGFR was found in a number of cancers (e.g., breast), their expression levels often correlate with vascularity, and is associated with poor prognosis in patients [25]. Inhibitors of the VEGFRTK are, therefore, expected to have great therapeutic potential in the treatment of malignant tumors.

We report here the synthesis of some new quinoline derivatives **6–12** and pyrimido[4,5-*b*]quinoline derivatives **16–20** to evaluate their anticancer activity against a human breast cancer cell line (MCF7). We also aimed to evaluate the ability of compounds **6** and **7** to enhance the cell killing effect of γ-radiation.

RESULTS AND DISCUSSION

Chemistry. Several compounds were designed with the aim of exploring their anticancer activity (Schemes 1–3). Enaminone **3** was obtained through condensation of 5,5-dimethyl-1,3-cyclohexandione **1** with *p*-bromoaniline **2**. The structure of compound **3** was supported by elemental analysis and spectral data. IR spectrum of compound **3** revealed the presence of bands at 3203 cm^{-1} (NH), 3091 cm^{-1} (CH arom.), at 2978, 2838 cm^{-1} (CH aliph.), and 1656 cm^{-1} (C=O). Treatment of enaminone **3** with 2-(4-methylbenzylidene)malononitrile **4** in ethanol containing a catalytic amount of triethylamine, as a base catalyst, yielded the corresponding hexahydroquinoline derivative **6** via the formation of the intermediate Michael type product **5** followed by intramolecular cyclization. IR spectrum of compound **6** revealed bands at 3311, 3203 cm^{-1} (NH_2), 2179 cm^{-1} (C≡N), 1656 cm^{-1} (C=O). The mass spectrum of **6** revealed a molecular ion peak *m/z* at 461 (M^+, 20.36%), with a base peak *m/z* at 372 (100) (Scheme 1).

Reaction of compound **6** with acetic anhydride under reflux condition for 10 h, afforded diacetyl derivative **7a** rather than monoacetyl form **7b** and cyclic system **7c**. IR spectrum of compound **7** showed band at 2208 cm^{-1} for (C≡N) and bands at 1700, 1658 cm^{-1} for (2C=O), whereas the ^{1}H-NMR spectrum of compound **7** revealed one singlet at 2.4 ppm of the acetyl groups. Interaction of compound **6** with concentrated sulfuric acid at room temperature caused partial hydrolysis of the cyano group yielding the corresponding amide derivative **8**, which was confirmed by the disappearance of the cyano group in the IR spectrum and presence of two carbonyl groups at 1678, 1648 cm^{-1}. ^{1}H-NMR spectrum showed the presence of singlet at 4.8 ppm for NH_2 group, and at 6.2 ppm for the $CONH_2$ group. Refluxing compound **6** in triethylorthoformate furnished the formimidate derivative **9**, which showed the absence of bands corresponding to the NH_2 group in the IR spectrum. Also, the ^{1}H-NMR spectrum showed the presence of significant triplet at 1.1 ppm for the CH_3, quartet at 3.9 ppm of CH_2 of the ethyl group and singlet corresponding to one proton of the

Scheme 2

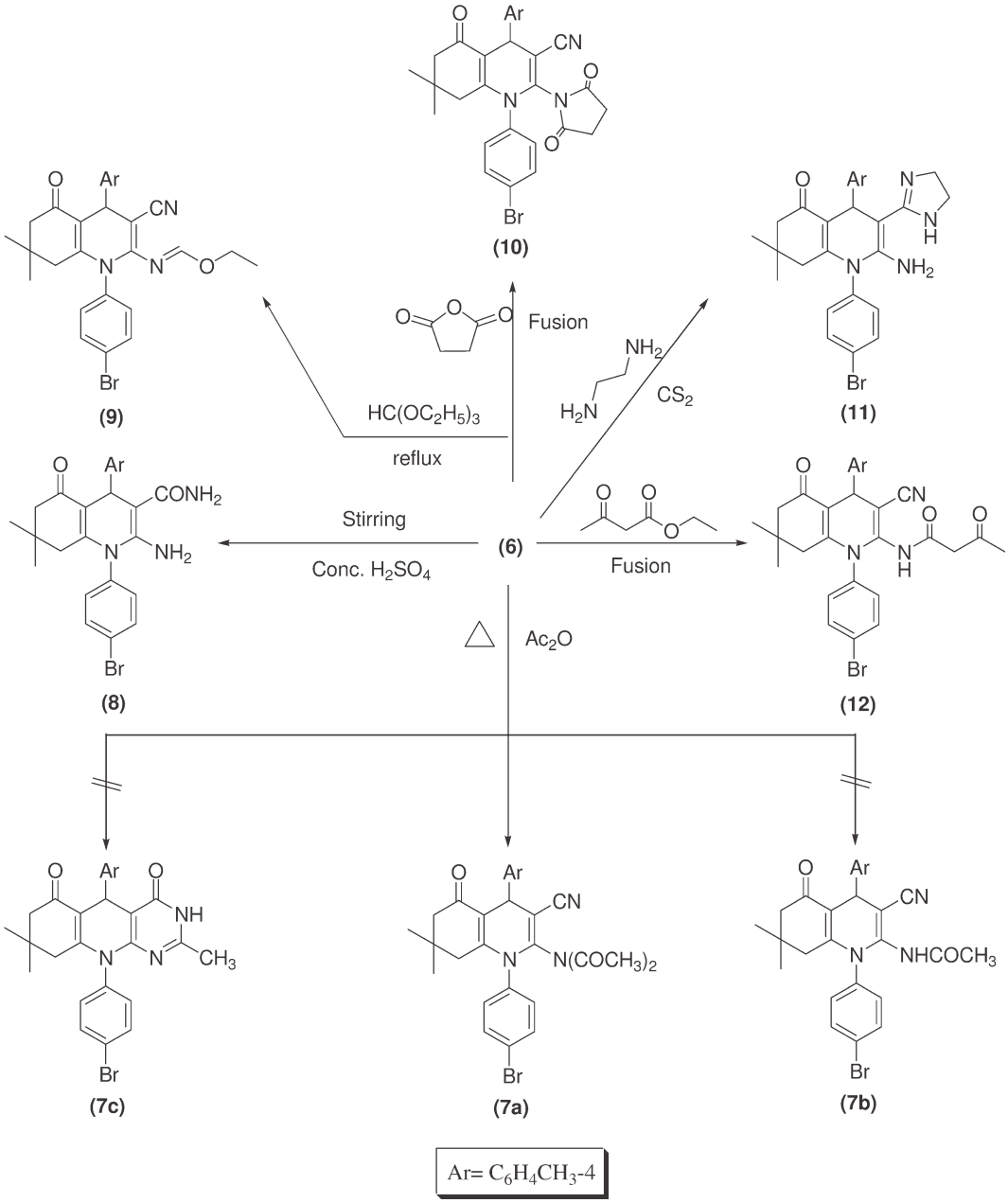

N=CH at 8.1 ppm. Fusion of compound **6** with succinic anhydride resulted pyrrolidine derivative **10**. IR spectrum of compound **10** revealed the presence of bands at 1794, 1733, 1668 cm^{-1} attributed to carbonyl groups. Mass spectrum of compound **10** exhibited a molecular ion peak at *m/z* 545 (M^+, 8.09%) and a base peak at *m/z* 77. The imidazolyl derivative **11** was obtained by refluxing compound **6** with ethylenediamine in the presence of carbon disulfide as a catalyst for 6 h. The reaction proceeded via intramolecular cyclization through the elimination of 1 mol of ammonia. Structure of compound **11** was established on the basis of elemental analysis and spectral data. IR spectrum of compound **11** revealed the absence of (C≡N) band. Additionally, its mass spectrum exhibited a molecular ion peak at *m/z* 504 (M^+, 6.34%) with a base peak at *m/z* 86. The 2-(3-oxobutanamido)quinoline derivative **12** was obtained via refluxing of compound **6** with ethyl acetoacetate. The reaction proceeded via the elimination of 1 mol of ethanol. IR spectrum of compound **12** revealed the presence of three carbonyl groups at (1840, 1728, and 1662 cm^{-1}). ^{1}H-NMR spectrum of compound **12** showed a singlet at 2.4 ppm for $COCH_3$, singlet at 4.8 ppm for $COCH_2$ and singlet at 10.1 ppm corresponding to NH (Scheme 2).

Scheme 3

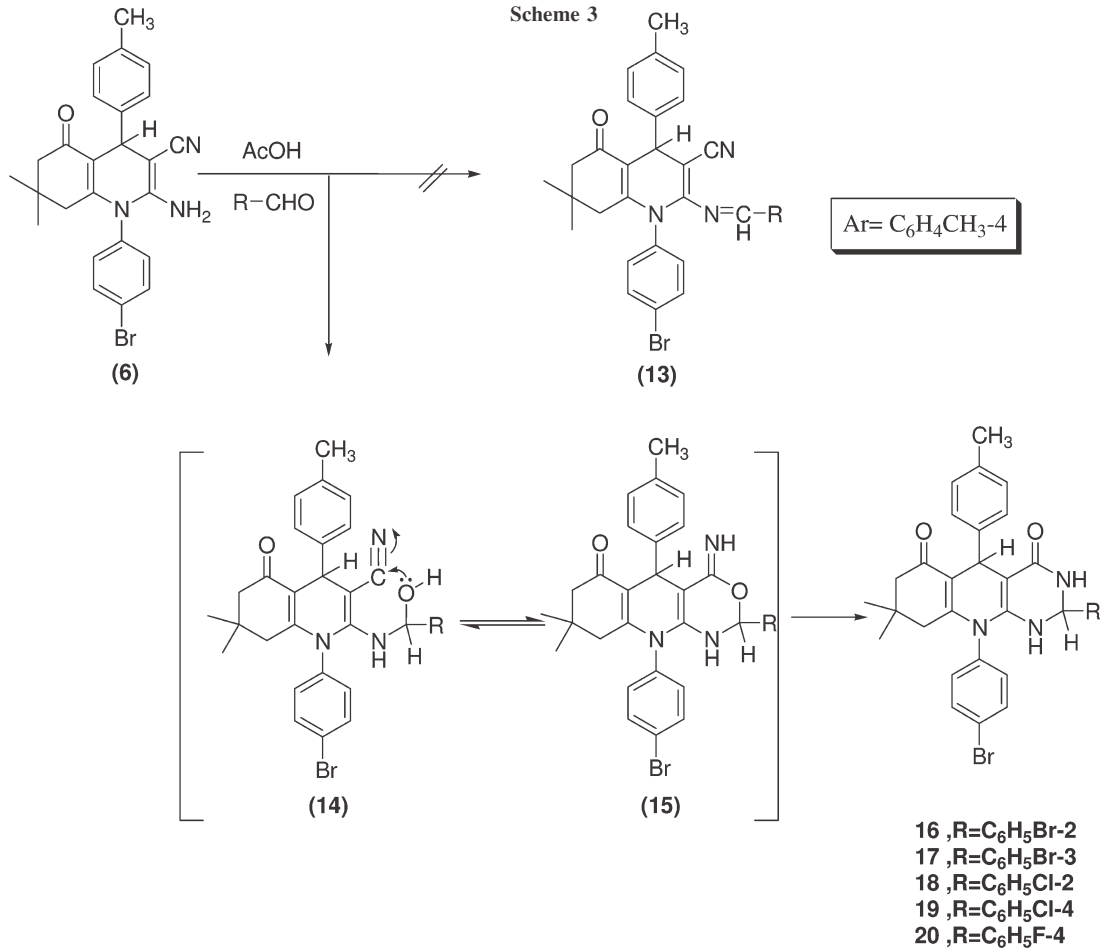

Reaction of compound **6** with aromatic aldehydes in acetic acid was expected to yield the corresponding Schiff's bases **13**. Although, what actually happened was an intramolecular cyclization via initial formation of intermediates **14**, **15** followed by a rearrangement to give the pyrimido[4,5-*b*]quinoline derivatives **16–20**. The structure of these compounds was proved on the bases of elemental analyses and IR spectrum which showed the absence of (C≡N) group and the presence of two bands corresponding to two carbonyl groups ranging from (1710–1658 cm^{-1}) of compounds **16–20**. Mass spectrum of compound **16** exhibited a molecular ion peak at *m/z* 645 (M^+, 2.08%) with a base peak at *m/z* 183, mass spectrum of compound **17** exhibited a molecular ion peak at *m/z* 645 (M^+, 4.46%) with a base peak at *m/z* 44, mass spectrum of compound **18** exhibited a molecular ion peak at *m/z* 603 (M^+, 10.68%) with a base peak at *m/z* 43, mass spectrum of compound **19** exhibited a molecular ion peak at *m/z* 600 (M^+, 1.4%) with a base peak at *m/z* 55 and mass spectrum of compound **20** exhibited a molecular ion peak at *m/z* 589 (M^+, 8.4%) with a base peak at *m/z* 43. ^{1}H-NMR spectrum of compound **19** showed a doublet at 4.9 ppm for NH pyrimidine, at 8.0 ppm for NHCO, and singlet at 6.1 ppm for CH pyrimidine (Scheme 3).

***In vitro* anticancer screening.** All the newly synthesized compounds were evaluated for their *in vitro* cytotoxic activity against human breast cancer cell line, MCF7. Doxorubicin, the reference drug used in this study, is one of the most effective antitumor agents used to produce regressions in acute leukemia's, Hodgkin's disease, and other lymphomas. The relationship between surviving fraction and drug concentration was plotted to obtain the survival curve of human breast cancer cell line (MCF7). The response parameter calculated was the IC_{50} value, which corresponds to the concentration required for 50% inhibition of cell viability. Table 1 shows the *in vitro* cytotoxic activity of the synthesized compounds, where some compounds exhibited significant activity compared with the reference drug. From Table 1, we can observe that the quinoline derivative **6** (IC_{50} = 8.5 μ*M*) and the diacetyl form of quinoline derivative **7** (IC_{50} = 21.9 μ*M*) exhibited a remarkable cytotoxic activity when compared with the

Table 1

In vitro anticancer screening of the newly synthesized compounds **(6–20)** against human breast cancer cell line (MCF7) .

	Compound concentration (μ*M*)				
	10	25	50	100	
Compound	Surviving fraction (Mean ± SE)[a]				IC_{50} (μ*M*)
Doxorubicin	0.451 ± 0.02	0.352 ± 0.02	0.290 ± 0.01	0.280 ± 0.03	32.02
6	0.276 ± 0.01	0.130 ± 0.03	0.176 ± 0.01	0.143 ± 0.01	8.5
7	0.561 ± 0.01	0.167 ± 0.01	0.102 ± 0.01	0.205 ± 0.01	21.9
8	0.525 ± 0.03	0.436 ± 0.07	0.163 ± 0.01	0.250 ± 0.01	33.1
9	0.904 ± 0.03	0.685 ± 0.01	0.355 ± 0.01	0.209 ± 0.01	53
10	0.819 ± 0.01	0.425 ± 0.02	0.119 ± 0.01	0.208 ± 0.01	38.6
11	0.816 ± 0.01	0.738 ± 0.04	0.253 ± 0.01	0.264 ± 0.01	52.3
12	0.921 ± 0.01	0.171 ± 0.01	0.158 ± 0.01	0.246 ± 0.01	36.73
16	0.643 ± 0.01	0.523 ± 0.01	0.264 ± 0.02	0.174 ± 0.01	40.1
17	0.872 ± 0.01	0.579 ± 0.01	0.394 ± 0.04	0.173 ± 0.01	38.3
18	0.952 ± 0.01	0.657 ± 0.01	0.359 ± 0.01	0.197 ± 0.01	52.8
19	0.812 ± 0.02	0.473 ± 0.01	0.232 ± 0.01	0.245 ± 0.01	44.4
20	0.808 ± 0.3	0.541 ± 0.04	0.238 ± 0.01	0.354 ± 0.01	50.8

[a] Each value is the mean of three values ± standard error.

reference drug doxorubicin (IC_{50} = 32.02 μ*M*). Although compound **8** (IC_{50} = 33.1 μ*M*) is nearly as active as doxorubicin.

Radiosensitizing evaluation. The rationale for combining chemotherapy and radiotherapy is based mainly on two ideas, one being spatial cooperation, which is effective if chemotherapy is sufficiently active to eradicate subclinical metastases and if the primary local tumor is effectively treated by radiotherapy. In this regard, no interaction between radiotherapy and chemotherapy is required. The other idea is the enhancement of radiation effects by direct enhancement of the initial radiation damage by incorporating drugs into DNA, inhibiting cellular repair, accumulating cells in a radiosensitive phase or eliminating radioresistant phase cells, eliminating hypoxic cells, or inhibiting the accelerated repopulation of tumor cells. Virtually, all chemotherapeutic agents have the ability to sensitize cancer cells to the lethal effects of ionizing radiation [26]. Consequently, the tendency of the most two active compounds **6** and **7**, to improve the cell killing effect of γ-irradiation, was studied. From the results obtained in Table 1, compound **6** showed an *in vitro* cytotoxic activity with IC_{50} value of 8.5 μ*M*, when the cells were subjected to different concentrations of the compound alone. Although when the cells were subjected to the same concentrations of compound **6**, and irradiated with a single dose of γ-radiation at a dose level of 8 Gy, as shown in Table 2, the IC_{50} value was synergistically decreased to 1.57 μ*M* (Fig. 1). Similarly, compound **7** showed IC_{50} value of 21.9 μ*M* when used alone, as shown in Table 1. The IC_{50} values were decreased to 3.14 μ*M* after irradiation (Fig. 2).

Molecular modeling. ***Generation of VEGFRTK inhibitor hypothesis using CATALYST software.*** The lead compounds **I–IV**, which were reported to have selective VEGFRTK inhibitory activity, were used to generate common feature hypothesis of VEGFRTK inhibitor (Fig. 3) [27]. The generated pharmacophore consisted of five features with constraint dimensions (Fig. 4).

Table 2

In vitro anticancer screening of compounds **6** and **7** against human breast cancer cell line (MCF7) in combination with γ-radiation.

			Compound concentration (μ*M*) + irradiation (8 Gy)				
			10	25	50	100	
Compd. no.	Control	Irradiated (8 Gy)	Surviving fraction (Means ± SE)[a]				IC_{50} (μ*M*)
6	1.000	0.927 ± 0.02*	0.147 ± 0.01*	0.082 ± 0.04*	0.036 ± 0.01*	0.021 ± 0.01*	1.57
7	1.000	0.927 ± 0.02*	0.193 ± 0.04*	0.134 ± 0.01*	0.084 ± 0.01*	0.065 ± 0.01*	3.14

[a] Each value is the mean of three values ± standard error.
* $P < 0.001$.

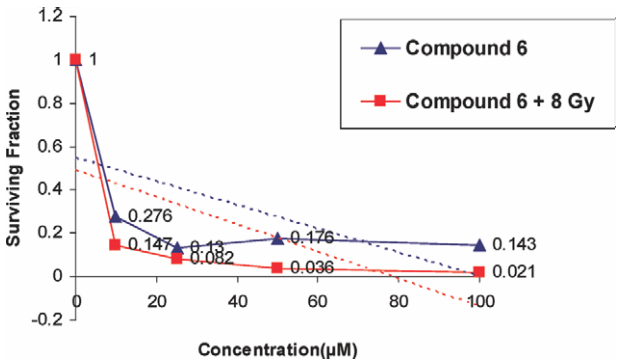

Figure 1. Survival curve for MCF7 cell line for compound **6** alone or in combination with γ-irradiation (8 Gy). [Color figure can be viewed in the online issue, which is available at wileyonlinelibrary.com.]

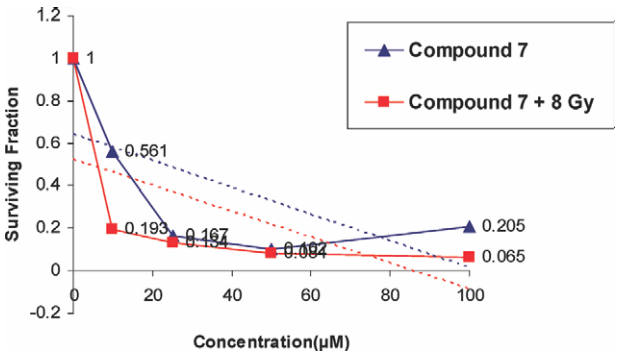

Figure 2. Survival curve for MCF7 cell line for compound 7 alone or in combination with γ-irradiation (8 Gy). [Color figure can be viewed in the online issue, which is available at wileyonlinelibrary.com.]

i.. Two hydrogen bond acceptor (HBA) appeared as a vector (green spherical mesh).
ii.. Three hydrophobic functions (HY1, HY2, and HY3) (blue spherical meshes).

Molecular modeling simulation studies were then conducted by measuring the compare/fit values, separately, between the conformational models of lead Vatalanib, compounds **6–20**, and ideal selective VEGFRTK inhibitor hypothesis (Fig. 5). The results of the best fitting values as well as the conformational energy of the best-fitted conformer with this hypothesis are given in Table 3. The results of simulation studies have revealed that compounds **6**, **8**, **11**, and **17–20** were filtered during mapping process, so they might act with another mechanism other than VEGFRTK inhibition. On the other hand, compound **7**, **10**, **12**, and **16** showed a remarkable fit values with a considerable IC_{50}, so these compounds might be promising anticancer molecules targeting VEGFRTK.

Docking studies. Regarding Vatalanib, four clusters of docked conformations were obtained, the largest cluster (four poses) was the lowest in mean docked energy, and the best member (in terms of docking score) was selected as the docked solution for Vatalanib, examination of the docking pose shows that Vatalanib forms two hydrogen bonds, one with Lys868 through its chlorine atom in benzene ring and the other

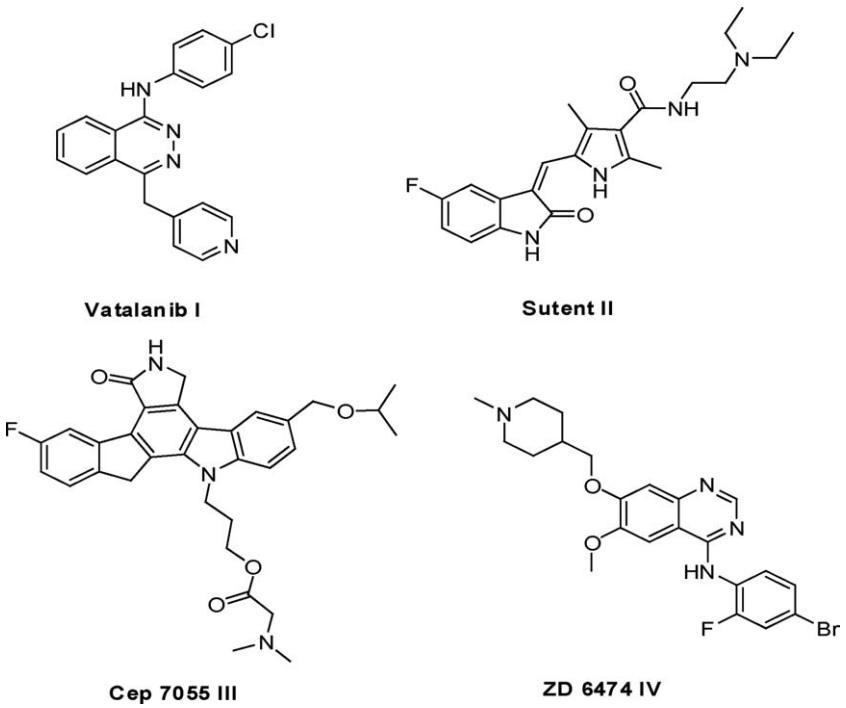

Figure 3. Structures of selective VEGFRTK inhibitory lead compounds **I–IV** used for generation of common feature VEGFRTK inhibitor hypothesis.

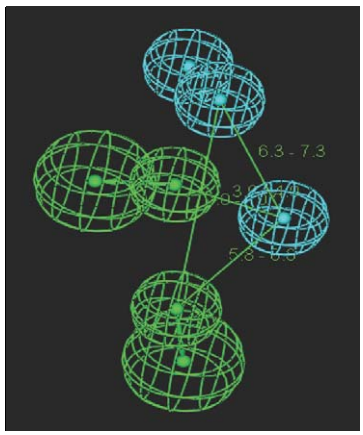

Figure 4. Generated hypothesis for VEGFRTK inhibitors with five features [three HY (pale blue) and two HBA (green)] with constraint distances and torsion angel of VEGFRTK hypothesis. [Color figure can be viewed in the online issue, which is available at wileyonlinelibrary.com.]

with Arg1032 through its nitrogen atom in phthalazine ring (Fig. 6). Using the RMSD tolerance of 1 Å, compound **7** gave 10 distinct clusters. The best pose of compound **7** showed good mapping to the docked pose of Vatalanib, its docking pose shows that formation of a hydrogen bond with Lys868 through its cyclohexanone oxygen atom (Fig. 7).

CONCLUSIONS

As breast cells are known to overexpress VEGFR, which leads to continuous activation of the VEGFR pathway involved in cell proliferation; therefore, we measured antitumor activity of the compounds in vitro on human breast carcinoma cell line (MCF-7). Two of the tested compounds exhibited potent inhibitory activity against MCF-7 cell line compared with other tested compounds and doxorubicin as a reference drug which are quinoline derivatives **6** and the diacetylated form **7**. Additionally, compound **8** is nearly as active as doxorubicin. Because it was reported that quinoline derivatives may exhibit potent VEGFRTK inhibition activity, which is considered to be an interesting target for the design of anticancer agents, the results obtained from the anticancer screening may give a suggestion that some of the synthesized compounds may act as VEGFRTK inhibitors and this may contribute in part to their anticancer activity. Docking studies revealed that compound **7** showed binding mode similar to Vatalanib, which was reported to have VEGFRTK inhibitory effects. Moreover, the most two active compounds **6** and **7** showed the ability to sensitize cancer cells to the lethal effects of ionizing radiation.

EXPERIMENTAL

Melting points are (°C, uncorrected) and were determined on Buchi melting point apparatus (B-540). Elemental analyses (C, H, and N) were performed on Perkin-Elmer 2400 analyser (Perkin-Elmer, Norwalk, CT) at Microanalytical Laboratories of the Faculty of Science, Cairo University. All compounds were within ±0.4% of the theoretical values. The IR spectra were measured on Nicolet 380 FTIR spectrometer. ^{1}H-NMR spectra were obtained on a Bruker proton NMR-Avance 300 (300, MHZ), in dimethyl sulfoxide (DMSO)-$d_6$as a solvent, using tetramethylsilane (TMS) as internal standard. Splitting patterns were designated as follows: s: singlet; d: doublet; t: triplet; m: multiplet. Mass spectra were run on HP Model MS-5988 (Hewlett Packard).

3-(4-Bromophenylamino)-5,5-dimethylcyclohex-2-enone 3. A mixture of 5,5-dimethylcyclohexane-1,3-dione **1** (1.4 g, 0.01 mol) and 4-bromoaniline **2** (1.7 g, 0.01 mol) in ethanol (20 mL) was refluxed for 5 h. The reaction mixture was cooled then poured onto cold water. The obtained solid was separated and crystallized from dioxane to give **3**. Yield, 79%; m.p. 128–130°C; IR (KBr, cm^{-1}): 3203 (NH), 3099 (CH arom.), 2978, 2838 (CH aliph.), 1656 (C=O). Anal. Calcd. for

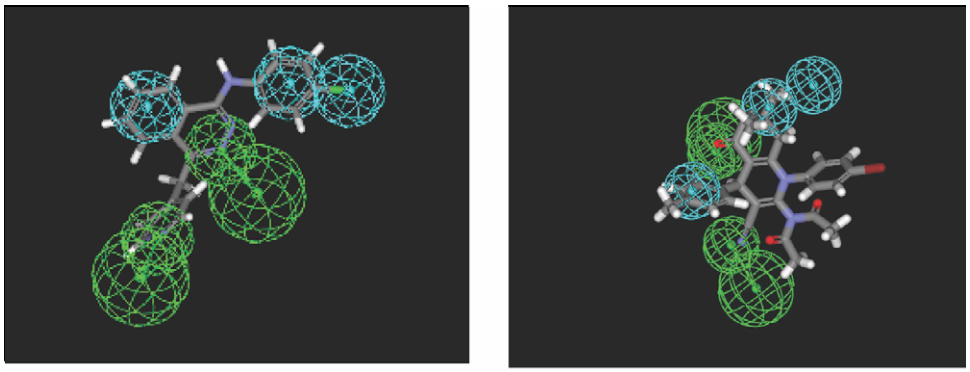

Figure 5. Mapping of VEGFRTK inhibitor hypothesis with Vatalanib and compound 7. [Color figure can be viewed in the online issue, which is available at wileyonlinelibrary.com.]

Table 3

Fit and energy values of some newly synthesized compounds in a comparison with Vatalanib.

Compound	Absolute energy (k/cal^{-1})	Fit value
7	124.189	3.073
9	121.354	3.31
10	112.509	3.421
12	101.164	3.50
16	80.02	3.555
Vatalanib	74.243	3.925

$C_{14}H_{16}BrNO$: C, 57.16; H, 5.48; N, 4.76. Found: C, 57.50; H, 5.10; N, 4.40.

2-Amino-1-(4-bromophenyl)-7,7-dimethyl-5-oxo-4-*p*-tolyl-1,4,5,6,7,8-hexahydroquinoline-3-carbonitrile 6. A mixture of compound **3** (2.94 g, 0.01 mol) and 2-(4-methylbenzylidene)malononitrile **4** (1.68 g, 0.01 mol) in ethanol (20 mL) containing three drops of triethylamine was refluxed for 6 h. The reaction mixture was filtered, whereas hot and the solid product was recrystallized from dioxane to give **6**. Yield, 75%; m.p. 262–264°C; IR (KBr, cm^{-1}): 3311, 3203 (NH_2), 3099 (CH arom.), 2978, 2838 (CH aliph.), 2179 (C≡N), 1656 (C=O). ^{1}H-NMR (DMSO-d_6) δ: 0.6, 0.9 [2s, 6H, $2CH_3$], 1.9–2.2 [m, 4H, $2CH_2$], 2.34 [s, 3H, CH_3 tolyl], 4.6 [s, 1H, CH], 5.4 [s, 2H, NH_2, D_2O exchangeable], 7.1–8.0 [m, 8H, Ar—H]. MS, *m*/*z* (%): 461 [M$^+$] (20.36), 372 (100). Anal. Calcd. for $C_{25}H_{24}BrN_3O$: C, 64.94; H, 5.23; N, 9.09. Found: C, 64.71; H, 5.10; N, 9.20.

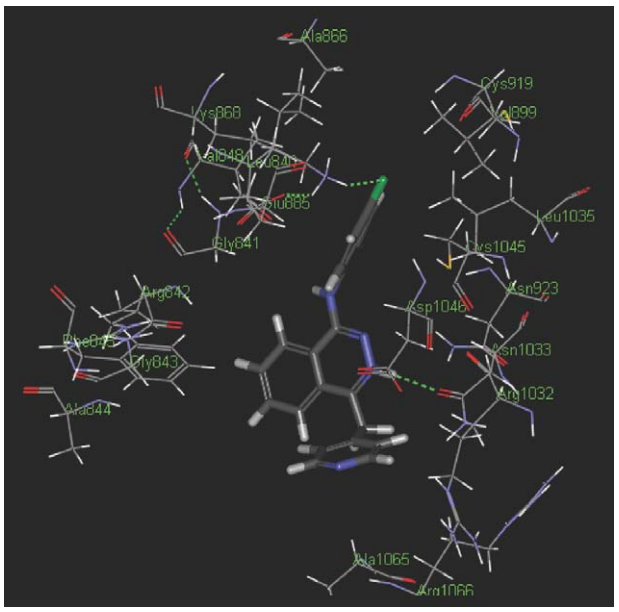

Figure 6. The proposed binding mode of Vatalanib inside the active site of VEGFRT kinase resulting from docking. The most important amino acids are shown together with their respective numbers. Vatalanib forms two hydrogen bonds, one with Arg1032 through its nitrogen (HB acceptor) in phthalazine moiety and the other with Lys868 through its chlorine atom in benzene ring. [Color figure can be viewed in the online issue, which is available at wileyonlinelibrary.com.]

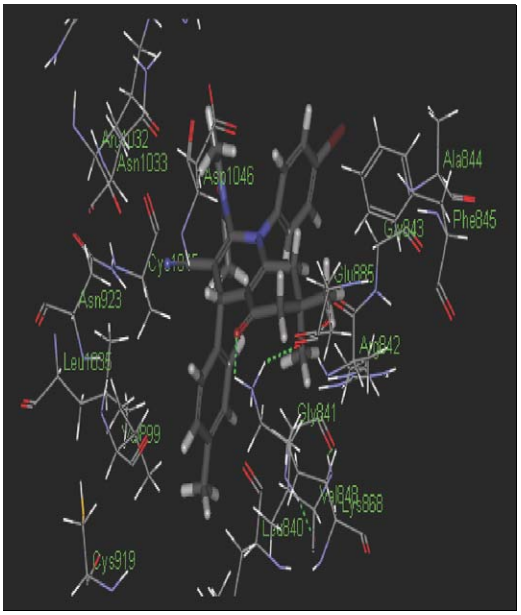

Figure 7. The proposed binding mode of compound 7 inside the active site of VEGFRT kinase resulting from docking. The most important amino acids is shown together with their respective numbers. Compound 7 forms one hydrogen bond with Lys868 through its oxygen atom in cyclohexanone ring. [Color figure can be viewed in the online issue, which is available at wileyonlinelibrary.com.]

***N*-acetyl-*N*-(1-(4-bromophenyl)-3-cyano-7,7-dimethyl-5-oxo-4-*p*-tolyl-1,4,5,6,7,8-hexahydroquinolin-2-yl)acetamide 7.** A solution of compound **6** (4.61 g, 0.01 mol) in acetic anhydride (30 mL) was refluxed for 10 h. The reaction mixture was then concentrated and the solid separated was recrystallized from ethanol to give **7**. Yield, 36 %; m.p. 120–122°C; IR (KBr, cm^{-1}): 3090 (CH arom.), 2928, 2880 (CH aliph.), 2208 (C≡N), 1700, 1658 (2C=O). MS, *m*/*z* (%): 545 [M$^+$] (2.04), 78 (100). ^{1}H-NMR (DMSO-d_6) δ: 0.7, 0.9 [2s, 6H, $2CH_3$], 1.8–2.2 [m, 4H, $2CH_2$], 2.3 [s, 3H, CH_3 tolyl], 2.4 [s, 6H, $2COCH_3$], 4.6 [s, 1H, CH], 7.0–7.7 [m, 8H, Ar—H]. Anal. Calcd. for $C_{29}H_{28}BrN_3O_3$: C, 63.74; H, 5.23; N, 7.69. Found: C, 63.40; H, 5.10; N, 7.49.

2-Amino-1-(4-bromophenyl)-7,7-dimethyl-5-oxo-4-*p*-tolyl-1,4,5,6,7,8-hexahydroquinoline-3-carboxamide 8. A solution of compound **6** (4.61 g, 0.01 mol) in concentrated H_2SO_4 (10 mL) was stirred for 6 h at room temperature. The reaction mixture was then poured onto ice cold water. The obtained solid was recrystallized from ethanol to give **8**. Yield, 66 %; m.p. 172–174°C; IR (KBr, cm^{-1}): 3385, 3182 (NH_2), 3052 (CH arom.), 2937, 2850 (CH aliph.), 1678, 1648 (2C=O). ^{1}H-NMR (DMSO-d_6) δ: 0.6, 0.9 [2s, 6H, $2CH_3$], 1.8–2.2 [m, 4H, $2CH_2$], 2.3 [s, 3H, CH_3 tolyl], 4.6 [s, 1H, CH], 4.8 [s, 2H, NH_2, D_2O exchangeable], 6.2 [s, 2H, $CONH_2$], 7.0–8.0 [m, 8H, Ar—H]. Anal. Calcd. for $C_{25}H_{26}BrN_3O_2$: C, 62.50; H, 5.46; N, 8.75. Found: C, 62.15; H, 5.89; N, 8.54.

(*E*)-ethyl *N*-1-(4-bromophenyl)-3-cyano-7,7-dimethyl-5-oxo-4-*p*-tolyl-1,4,5,6,7,8-hexahydroquinolin-2-ylformimidate 9. A solution of compound **6** (4.61 g, 0.01 mol) in triethylorthoformate (10 mL) was refluxed for 8 h. The reaction mixture was cooled and then poured onto ice water. The solid precipitate

was filtered and recrystallized from ethanol to give **9**. Yield, 81%; m.p. 190–192°C; IR (KBr, cm^{-1}): 3052 (CH arom.), 2959, 2890 (CH aliph.), 2208 (C≡N), 1632 (C=O). ^{1}H-NMR (DMSO-d_6) δ: 0.6, 0.9 [2s, 6H, $2CH_3$], 1.1 [t, 3H, CH_3 ethyl], 1.9–2.2 [m, 4H, $2CH_2$], 2.3 [s, 3H, CH_3 tolyl], 3.9 [q, 2H, CH_2 ethyl], 4.6 [s, 1H, CH], 7.1–7.9 [m, 8H, Ar—H], 8.1 [s, 1H, N=CH]. Anal. Calcd. for $C_{28}H_{28}BrN_3O_2$: C, 64.87; H, 5.44; N, 8.11. Found: C, 64.54; H, 5.13; N, 8.50.

1-(4-Bromophenyl)-2-(2,5-dioxopyrrolidin-1-yl)-7,7-dimethyl-5-oxo-4-*p*-tolyl-1,4,5,6,7,8-hexahydroquinoline-3-carbonitrile 10. A mixture of compound **6** (4.61 g, 0.01 mol) and succinic anhydride (1 g, 0.01 mol) was fused together in an oil bath at 250°C for 15 min, athe fused mass was dissolved in dimethylformamide and poured onto ice cold water, and the solid obtained was crystallized from ethanol to give **10**. Yield, 47%; m.p. 144–146°C; IR (KBr, cm^{-1}): 3085 (CH arom.), 2960, 2880 (CH aliph.), 2213 (C≡N), 1794, 1733, 1668 (3C=O). ^{1}H-NMR (DMSO-d_6) δ: 0.7, 0.9 [2s, 6H, $2CH_3$], 1.9–2.2 [m, 4H, $2CH_2$], 2.3 [s, 3H, CH_3 tolyl], 4.8 [s, 1H, CH], 5.2 [t, 4H, $2CH_2$ pyrrolidine, J = 6.2 Hz], 7.0–8.0 [m, 8H, Ar—H]. MS, m/z (%): 545 [M^+] (8.09), 77 (100). Anal. Calcd. for $C_{27}H_{26}BrN_3O_3$: C, 63.98; H, 4.81; N, 7.72. Found: C, 63.78; H, 4.61; N, 7.52.

2-Amino-1-(4-bromophenyl)-3-(4,5-dihydro-1H-imidazol-2-yl)-7,7-dimethyl-4-*p*-tolyl-4,6,7,8-tetrahydroquinolin-5(1H)-one 11. A solution of compound **6** (4.61 g, 0.01 mol) and ethylenediamine (7 mL) was refluxed in carbon disulfide (10 mL) for 6 h. The reaction mixture was cooled and then poured onto ice cold water. The solid obtained was crystallized from dioxane to give **11**. Yield, 55%; m.p. 108–110°C; IR (KBr, cm^{-1}), 3271, 3225 (NH, NH_2), 3033 (CH arom.), 2919, 2850 (CH aliph.), 1675 (C=O). ^{1}H-NMR (DMSO-d_6) δ: 0.9, 1.0 [2s, 6H, $2CH_3$], 1.9–2.2 [m, 4H, $2CH_2$], 2.3 [s, 3H, CH_3 tolyl], 4.5 [s, 1H, CH], 5.6 [s, 2H, NH_2, D_2O exchangeable], 6.4–6.6 [m, 4H, $2CH_2$ imidazole], 7.1–8.0 [m, 8H, Ar—H]. MS, m/z (%): 504 [M^+] (6.34), 86 (100). Anal. Calcd. for $C_{27}H_{29}BrN_4O$: C, 64.94; H, 5.16; N, 11.08. Found: C, 64.71; H, 5.46; N, 11.30.

***N*-(1-(4-bromophenyl)-3-cyano-7,7-dimethyl-5-oxo-4-*p*-tolyl-1,4,5,6,7,8-hexahydroquinolin-2-yl)-3-oxobutanamide 12.** A solution of compound **6** (4.61 g, 0.01 mol) in ethyl acetoacetate (10 mL) was refluxed for 5 h. The reaction mixture was then concentrated, the solid separated was crystallized from ethanol to give **12**. Yield, 91%; m.p. 47–49°C; IR (KBr, cm^{-1}): 3204 (NH), 3080 (CH arom.), 2959, 2833 (CH aliph.), 2210 (C≡N), 1840, 1728, 1662 (3C=O). ^{1}H-NMR (DMSO-d_6) δ: 0.7, 0.9 [2s, 6H, $2CH_3$], 1.9–2.1 [m, 4H, $2CH_2$], 2.3 [s, 3H, CH_3 tolyl], 2.4 [s, 3H, $COCH_3$], 4.5 [s, 1H, CH], 4.8 [s, 2H, $COCH_2$], 7.1–7.9 [m, 8H, Ar—H], 10.1 [s, 1H, NH]. Anal. Calcd. for $C_{29}H_{28}BrN_3O_3$: C, 63.74; H, 5.16; N, 7.69. Found: C, 63.90; H, 5.45; N, 7.39.

2-(Substituted)-10-(4-bromophenyl)-8,8-dimethyl-5-*p*-tolyl-2,3,7,8,9,10-hexahydropyrimido[4,5-*b*]quinoline-4,6(1H,5H)-dione 16–20. A mixture of **6** (4.61 g, 0.01 mol) and aromatic benzaldehydes (0.01 mol) in acetic acid (20 mL) was refluxed for 5 h. The reaction mixture was cooled then poured onto ice cold water where a precipitate was formed. The precipitate was filtered and crystallized from dioxane to give **16–20**, respectively.

***2-(2-Bromophenyl)-10-(4-bromophenyl)-8,8-dimethyl-5-*p*-tolyl-2,3,7,8,9,10-hexahydropyrimido[4,5-*b*]quinoline-4,6(1H,5H)-dione 16*.** Yield, 74%; m.p. 100–102°C; IR (KBr, cm^{-1}): 3390 (NH), 3080 (CH arom.), 2956, 2876 (CH aliph.), 1707, 1657 (2C=O). MS, m/z (%): 645 [M^+] (2.08), 183 (100). Anal. Calcd. for $C_{32}H_{29}Br_2N_3O_2$: C, 59.37; H, 4.52; N, 6.49. Found: C, 59.66; H, 4.99; N, 6.89.

***2-(3-Bromophenyl)-10-(4-bromophenyl)-8,8-dimethyl-5-*p*-tolyl-2,3,7,8,9,10-hexahydropyrimido[4,5-*b*]quinoline-4,6(1H,5H)-dione 17*.** Yield, 74%; m.p. 88–90°C; IR (KBr, cm^{-1}): 3390 (NH), 3080 (CH arom.), 2956, 2876 (CH aliph.), 1707, 1657 (2C=O). MS, m/z (%): 645 [M^+] (4.46),) 44 (100). Anal. Calcd. for $C_{32}H_{29}Br_2N_3O_2$: C, 59.37; H, 4.52; N, 6.49. Found: C, 59.61; H, 4.92; N, 6.93.

***10-(4-Bromophenyl)-2-(2-chlorophenyl)-8,8-dimethyl-5-*p*-tolyl-2,3,7,8,9,10-hexahydropyrimido[4,5-*b*]quinoline-4,6(1H,5H)-dione 18*.** Yield, 74%; m.p. 72–74°C; IR (KBr, cm^{-1}): 3390 (NH), 3080 (CH arom.), 2956, 2876 (CH aliph.), 1707, 1657 (2C=O). MS, m/z (%): 603 [M^+] (10.68), 43 (100). Anal. Calcd. for $C_{32}H_{29}BrClN_3O_2$: C, 63.74; H, 4.85; N, 6.97. Found: C, 63.22; H, 4.35; N, 6.50.

***10-(4-Bromophenyl)-2-(4-chlorophenyl)-8,8-dimethyl-5-*p*-tolyl-2,3,7,8,9,10-hexahydropyrimido[4,5-*b*]quinoline-4,6(1H,5H)-dione 19*.** Yield, 41%; m.p. 58–60°C; IR (KBr, cm^{-1}): 3390 (NH), 3080 (CH arom.), 2956, 2876 (CH aliph.), 1707, 1657 (2C=O). ^{1}H-NMR (DMSO-d_6) δ: 0.7, 0.9 [2s, 6H, $2CH_3$], 1.9–2.0 [m, 4H, $2CH_2$], 2.3 [s, 3H, CH_3 tolyl], 4.5 [s, 1H, CH], 4.9 [d, 1H, NH pyrimidine], 6.1 [s, 1H, CH pyrimidine], 7.1–7.9 [m, 8H, Ar—H], 8.0 [d, 1H, NHCO]. MS, m/z (%): 600 [M^+] (1.4), 55 (100). Anal. Calcd. for $C_{32}H_{29}BrClN_3O_2$: C, 63.74; H, 4.85; N, 6.97. Found: C, 63.29; H, 4.40; N, 6.53.

***10-(4-Bromophenyl)-2-(4-fluorophenyl)-8,8-dimethyl-5-*p*-tolyl-2,3,7,8,9,10-hexahydropyrimido[4,5-*b*]quinoline-4,6(1H,5H)-dione 20*.** Yield, 64%; m.p. 100–104°C; IR (KBr, cm^{-1}): 3390 (NH), 3080 (CH arom.), 2956, 2876 (CH aliph.), 1707, 1657 (2C=O). MS, m/z (%): 589 [M^+] (8.4), 43 (100). Anal. Calcd. for $C_{32}H_{29}BrFN_3O_2$: C, 65.53; H, 4.98; N, 7.16. Found: C, 65.53; H, 4.43; N, 7.56.

***In vitro* anticancer screening.** Human tumor breast cell line (MCF7) was used in this study. The cytotoxic activity was measured in vitro for the newly synthesized compounds using the Sulfo-Rhodamine-B stain (SRB) assay using the method of Skehan et al. [28]. The *in vitro* anticancer screening was done by the pharmacology unit at the National Cancer Institute, Cairo University.

Cells were plated in 96-multiwell microtiter plate (10^4cells/well) for 24 h before treatment with the compound(s) to allow attachment of cell to the wall of the plate. Test compounds were dissolved in DMSO and diluted with saline to the appropriate volume. Different concentrations of the compound under test (0, 10, 25, 50, and 100 μ*M*/mL) were added to the cell monolayer. Triplicate wells were prepared for each individual dose. Monolayer cells were incubated with the compound(s) for 48 h at 37°C and in humidified incubator with 5% CO_2. After 48 h, cells were fixed, washed, and stained for 30 min with 0.4% (wt/vol) SRB dissolved in 1% acetic acid. Excess unbounded dye was removed by four washes with 1% acetic acid, and attached stain was recovered with Tris ethylene diamine tetra-acetic acid (EDTA) buffer. Color intensity was measured in an enzyme-linked immunosorbent assay (ELISA) reader. The relation between surviving fraction and drug concentration is plotted to get the survival curve for human breast tumor cell line after the specified time. The molar concentration required for 50% inhibition of cell viability (IC_{50}) was

calculated and compared to the reference drug doxorubicin (CAS, 25316-40-9). The surviving fractions were expressed as means ± standard error and the results are given in Table 1.

Radiosensitizing evaluation. The most potent compounds resulted from the *in vitro* anticancer screening; the quinoline derivative **6** and the diacetyl form of quinoline derivative **7** were selected to be evaluated again for their *in vitro* anticancer activity alone and in combination with γ-radiation. This study was conducted to evaluate the ability of these compounds to enhance the cell killing effect of γ-radiation.

Cells were subjected to a single dose of γ-radiation at a dose level of 8 Gy with a dose rate of 2 Gy/min. Irradiation was performed in the National Cancer Institute, Cairo University, using Gamma cell-40 (^{60}Co) source.

The surviving fractions were expressed as means ± standard error. The results were analyzed using 1-way ANOVA test and given in Table 2.

COMPUTATIONAL DETAILS

Catalyst molecular modeling experiments. All molecular modeling work was performed on Silicon Graphic (SGI), Fuel workstation (500 MHz, R 14000 ATM processor, 512 MB memory) using the catalyst package of Molecular Simulation (version 4.8), under an IRIX 6.8 operating system, at the Faculty of Pharmacy, Ain Shams University. A generalized visualizer, confirm, info, HipHop, compare/fit, force field was used throughout.

Training sets, lead compounds **I–IV**, were selected. Molecules were built within the catalyst and conformational models for each compound were generated automatically using the poling algorithm. This emphasizes representative coverage over a 20 kcal mol^{-1} energy range above the estimated global energy minimum and the best searching procedure was chosen. The training molecules with their associated conformational models were submitted to catalyst by using default common features hypothesis generation by using HipHop commands. All needed features for VEGFRTK inhibitors were selected from the Dictionary List: HB acceptor, hydrophobic (HY), and HB donor. By this step, we specified the expected features required for the activity of VEGFRTK inhibitors. Then, a generate hypothesis order was given to the computer. Finally, the process data were collected, and the process log files were examined which showed that 10 hypotheses were generated. All the 10 generated hypotheses were analyzed. The assessment of the ideal hypothesis among the generated ones indicated that hypothesis ranked number 2 was the ideal one.

Docking studies. The docking was performed using Accelry's Discovery Studio 2.5.5 [29]. The docking was performed on two compounds: Vatalanib and **7**. The structures were minimized by Merck Molecular force field (MMFF) to a gradient of 4.5×10^{-5} using Spartan'06. The optimized geometries were exported as Sybyl mol2 file, which were exported to Discovery Studio tools. Gasteiger charges were calculated for each molecule and the torsional degrees of freedom were set to the maximum number of rotatable bonds. The receptor structure was downloaded from the protein databank (pdb) [www.rcsb.org], pdb entry 1VR2. Water molecules were deleted from the file and hydrogens were added, then Kollman charges were calculated. No further geometry optimization was performed. Nonpolar hydrogens were merged with the parent atoms for both the ligands and the receptor. The docking itself was performed using the Lamarckian Genetic Algorithm, with a translational increment of 0.5 Å, and both quaternion and torsional angles were incremented by 15 Å each. The generation size was set to 150 individuals per generation, and the rest of the docking parameters were kept to the default values. Ten runs of the genetic algorithm were performed, thus for each compound, we got 10 docked poses, which were subsequently clustered relative to the original MMFF structure using root mean square deviation (RMSD) tolerance of 1.0 Å. The poses were evaluated using the default empirical scoring function in Discovery Studio.

REFERENCES AND NOTES

[1] El-Gazzar, A. B.; Hafez, H. N.; Nawwar, G. A. Eur J Med Chem 2009, 44, 1427.

[2] Palit, P.; Paira, P.; Hazra, A.; Banerjee, S.; Gupta, A. D.; Dastidar, S. G.; Mondal, N. B. Bioorg Med Chem 2009, 14, 6475.

[3] Kategaonkar, A. H.; Pokalwar, R. U.; Sonar, S. S.; Gawali, V. U.; Shingate, B. B.; Shingare, M. S. Eur J Med Chem 2010, 45, 1128.

[4] Eswaran, S.; Adhikari, A. V.; Kumar, R. A. Eur J Med Chem 2010, 45, 957.

[5] Joshi, A. A.; Narkhede, S. S.; Viswanathan, C. L. Bioorg Med Chem Lett 2005, 15, 73.

[6] Milner, E.; McCalmont, W.; Bhonsle, J.; Caridha, D.; Carroll, D.; Gardner, S.; Gerena, L.; Gettayacamin, M.; Lanteri, C.; Luong, T.; Melendez, V.; Moon, J.; Roncal, N.; Sousa, J.; Tungtaeng, A.; Wipf, P.; Dow, G. Bioorg Med Chem Lett 2010, 20, 1347.

[7] Alqasoumi, S. I.; Al-Taweel, A. M.; Alafeefy, A. M.; Noaman, E.; Ghorab, M. M. Eur J Med Chem 2010, 45, 738.

[8] Behforouz, M.; Cai, W.; Mohammadi, F.; Stocksdale, M. G.; Gu, Z.; Ahmadian, M.; Baty, D. E.; Etling, M. R.; Al-Anzi, C. H.; Swiftney, T. M.; Tanzer, L. R.; Merriman, R. L.; Behforouz, N. C. Bioorg Med Chem 2007, 15, 495.

[9] Kemnitzer, W.; Kuemmerle, J.; Jiang, S.; Zhang, H.; Sirisoma, N.; Kasibhatla, S.; Grundy, C. C.; Tseng, L. B.; Drewe, J.; Cai, S. X. Bioorg Med Chem Lett 2008, 18, 6259.

[10] Ferlin, M. G.; Gatto, B.; Chiarelotto, G.; Palumbo, M. Bioorg Med Chem 2001, 9, 1843.

[11] Abouzid, K.; Shouman, S. Bioorg Med Chem 2008, 16, 7543.

[12] Gopal, M.; Shenoy, S.; Doddamani, L. S. J Photochem Photobiol B 2003, 72, 69.

[13] Kim, Y. H.; Shin, K. J.; Lee, T. G.; Kim, E.; Lee, M. S.; Ryu, S. H.; Suh, P. G. Biochem Pharmacol 2005, 69, 1333.

[14] Zhao, Y. L.; Chen, Y. L.; Chang, F. S.; Tzeng, C. C. Eur J Med Chem 2005, 40, 792.

[15] Cheng, Y.; An, L. K.; Wu, N.; Wang, X. D.; Bu, X. Z.; Huang, Z. S.; Gu, L. Q. Bioorg Med Chem 2008, 16, 4617.

[16] Alqasoumi, S. I.; Al-Taweel, A. M.; Alafeefy, A. M.; Hamed, M. M.; Noaman, E.; Ghorab, M. M. Bioorg Med Chem Lett 2009, 19, 6939.

[17] Mulvihill, M. J.; Ji, Q. S.; Coate, H. R.; Cooke, A.; Dong, H.; Feng, L.; Foreman, K.; Franklin, M. R.; Honda, A.; Mak, G.; Mulvihill, K. M.; Nigro, A. I.; O'Connor, M.; Pirrit, C.; Steinig, A. G.; Siu, K.; Stolz, K. M.; Sun, Y.; Tavares, P. A.; Yao, Y. Bioorg Med Chem 2008, 16, 1359.

[18] Nishii, H.; Chiba, T.; Morikami, K.; Fukami, T. A.; Sakamoto, H.; Ko, K.; Koyano, H. Bioorg Med Chem 2010, 20, 1405.

[19] Pannala, M.; Kher, S.; Wilson, N.; Gaudette, J.; Sircar, I.; Zhang, S.; Bakhirev, A.; Yang, G.; Yuen, P.; Gorcsan, F.; Sakurai, N.; Barbosa, M. J Bioorg Med Chem Lett 2007, 17, 5978.

[20] Kubo, K.; Shimizu, T.; Ohyama, S.; Murooka, H.; Iwai, A.; Nakamura, K.; Hasegawa, K.; Kobayashi, Y.; Takahashi, N.; Takahashi, K.; Kato, S.; Izawa, T.; Isoe, T. J Med Chem 2005, 48, 1359.

[21] Matsui, J.; Yamamoto, Y.; Funahashi, Y.; Tsuruoka, A.; Watanabe, T.; Wakabayashi, T.; Uenaka, T.; Asada, M. Int J Cancer 2008, 122, 664.

[22] Campas, C.; Bolos, J.; Castaner, R. Drugs Future 2009, 34, 793.

[23] Kamen, B. A.; Cole, P. D.; Bertino, J. R. In Cancer Medicine; Bast, R. C., Kufe, D. W., Pollock, R. E., Weichselbaum, R. R., Holland, J. F., Frei, B. C., Decke, E., Eds.; B.C. Decker Inc.: London, UK, 2000; Vol. 5, p 612.

[24] Tonini, T.; Rossi, F.; Claudio, P. P. Oncogene 2003, 22, 6549.

[25] Kurenova, E. V.; Hunt, D. L.; He, D.; Fu, A. D.; Massoll, N. A.; Golubovskaya, V. M.; Garces, C. A.; Cance, W. G. Cell cycle 2009, 15, 2868.

[26] Nishimura, Y. Int J Clin Oncol 2004, 9, 414.

[27] Calderwood, D. J.; Johnson, D. N.; Munschauer, R.; Rafferty, P. Bioorg Med Chem Lett 2002, 12, 1683.

[28] Skehan, P.; Storeng, R.; Scudiero, D.; Monks, A.; McMahon, J.; Vistica, D.; Warren, J. T.; Bokesch, H.; Kenney, S.; Boyd, M. R. J Natl Cancer Inst 1990, 82, 1107.

[29] Koska, J.; Spassov, V. Z.; Maynard, A. J.; Yan, L.; Austin, N.; Flook, P. K.; Venkatachalam, C. M. J Chem Inf Model 2008, 48, 1965.